Nanoscale

COMMUNICATION

View Article Online
View Journal | View Issue

Cite this: *Nanoscale*, 2024, **16**, 6442

Received 28th December 2023,
Accepted 29th February 2024

DOI: 10.1039/d3nr06626f

rsc.li/nanoscale

Transient control of lytic activity *via* a non-equilibrium chemical reaction system†

Kohei Sato, *‡§[a] Yume Nakagawa,‡[a] Miki Mori,[a] Masahiro Takinoue [a,b,c] and Kazushi Kinbara *[a,c]

The development of artificial non-equilibrium chemical reaction systems has recently attracted considerable attention as a new type of biomimetic. However, due to the lack of bioorthogonality, such reaction systems could not be linked to the regulation of any biological phenomena. Here, we have newly designed a non-equilibrium reaction system based on olefin metathesis to produce the Triton X-mimetic non-ionic amphiphile as a kinetic product. Using phospholipid vesicles encapsulating fluorescent dyes and red blood cells as cell models, we demonstrate that the developed chemical reaction system is applicable for transient control of the resulting lytic activity.

[a]*School of Life Science and Technology, International Research Frontiers Initiative, Tokyo Institute of Technology, 4259 Nagatsuta-cho, Midori-ku, Yokohama 226-8501, Japan. E-mail: ksato@kwansei.ac.jp, kkinbara@bio.titech.ac.jp*
[b]*Department of Computer Science, International Research Frontiers Initiative, Tokyo Institute of Technology, 4259 Nagatsuta-cho, Midori-ku, Yokohama 226-8501, Japan*
[c]*Living Systems Materialogy Research Group, International Research Frontiers Initiative, Tokyo Institute of Technology, 4259 Nagatsuta-cho, Midori-ku, Yokohama 226-8501, Japan*

†Electronic supplementary information (ESI) available. See DOI: https://doi.org/10.1039/d3nr06626f

‡These authors contributed equally to this work.

§Present address: Department of Chemistry, School of Science, Kwansei Gakuin University, 1 Gakuen Uegahara, Sanda-shi, Hyogo 669–1330, Japan.

Introduction

The development of life-like architectures has long been the ultimate goal in organic chemistry.[1–3] To date, remarkable advances in synthetic and supramolecular chemistry have enabled the construction of complex molecular assemblies reminiscent of natural biomacromolecules such as proteins[4–15] and nucleic acids.[16–22] More recently, the development of artificial systems that mimic the non-equilibrium chemical reactions in living organisms, known as systems chemistry, has attracted considerable attention as a new type of biomimetic.[23–32] Furthermore, such reactions have been associated with functional outcomes, for example, drug release,[33,34] modulation of chemical reactions,[35,36] and control

Kohei Sato

Kohei Sato received his PhD from the University of Tokyo in 2014 under the supervision of Professor Takuzo Aida. He then conducted postdoctoral research in the group of Professor Samuel I. Stupp at Northwestern University. In 2018, he joined the group of Professor Kazushi Kinbara as an assistant professor. In 2023, he started his independent career as an associate professor in the Department of Chemistry at Kwansei Gakuin University. His current research focuses on the development of bioactive supramolecular materials.

Yume Nakagawa

Yume Nakagawa was born in Mie, Japan in 1999. She completed her undergraduate course from the Tokyo Institute of Technology and is currently continuing her research as a postgraduate student in the Kinbara group. Her research interests are non-equilibrium chemical reactions, particularly in Systems Chemistry.

of the microscopic movement of colloids.[37] However, to the best of our knowledge, such reaction systems have never been involved in interacting directly with biomolecules to regulate any biological phenomena. Undoubtedly, non-equilibrium chemical reaction systems are highly advantageous for their promising potential to precisely and temporally control biological activities. However, conventional systems chemistry was mostly based on the reactions of polar functional groups,[38] including carboxylic acids for carbodiimide-fueled reactions,[39,40] amines for imine formation,[41,42] and thiols for thiol–ester and thiol–disulfide exchange reactions.[43–45] Because such polar functional groups are abundant in biomolecules, these reactions would most likely show interference under physiological conditions.

Recently, Fletcher and coworkers have developed non-equilibrium chemical reaction systems based on the ruthenium-catalyzed cross-metathesis of hydrophilic and hydrophobic alkenes.[46] Here, we took advantage of the bioorthogonality of the metathesis reaction[47–50] and sought to introduce a new molecular design strategy into Fletcher's system to promote direct interaction between the resulting product and biomolecules. The chemical structure of a well-known commercial synthetic surfactant, Triton X (Fig. 1), provided us with a clue. Triton X is a non-ionic amphiphile consisting of a hydrophobic aliphatic tail, an aromatic ring, and a hydrophilic poly(ethylene glycol) (PEG) chain, known for its high propensity to interact with lipid molecules to disrupt biomembranes while preventing protein denaturation.[51,52] Therefore, we designed a non-equilibrium chemical reaction system based on olefin metathesis to produce a Triton-mimetic amphiphile as a kinetic product. Through this study, we expected to establish a proof-of-concept system to realize the temporal control of biological activity synchronous to an artificial non-equilibrium chemical reaction. In particular, we focused on controlling the interaction with cell membranes (Fig. 1), the vital components of life.[3,53,54]

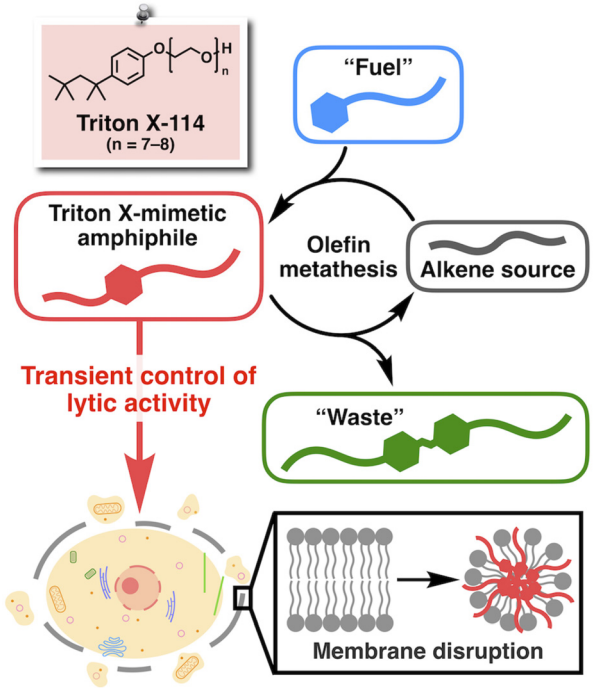

Fig. 1 Schematic illustrations of the chemical structure of Triton X-114 and a non-equilibrium chemical reaction system that produces the Triton-mimetic amphiphile as a kinetic product through olefin metathesis. The amphiphile was designed to interact with cell membranes to induce their disruption in a transient manner.

Results and discussion

The chemical structures of the reactants and products, and an overview of the chemical reaction system are shown in Fig. 2a. We selected 7-tetradecene as the alkene source of the hydrophobic moiety and designed a fuel alkene $^{\text{Fuel}}$**PEG** so that the

Masahiro Takinoue

Masahiro Takinoue is a biophysicist studying artificial cell engineering and molecular computing based on DNA nanotechnology. He received a B.Sc. in Physics in 2002, a M.Sc. in Physics in 2004, and a Ph.D. in Physics in 2007 from The University of Tokyo (UT), Japan. After serving as a postdoctoral fellow at Kyoto University and a project assistant professor at UT, he served as an associate professor at Tokyo Institute of Technology (Tokyo Tech), Japan (2011-2022). He has been a full professor at the Department of Computer Science and Living Systems Materialogy (LiSM) Research Group at Tokyo Tech (2022-).

Kazushi Kinbara

Dr. Kazushi Kinbara received a Ph.D. degree in organic chemistry from the University of Tokyo in 1996 under the direction of Professor Kazuhiko Saigo. From 2001, he joined Professor Takuzo Aida's group at School of Engineering, the University of Tokyo as a lecturer and associate professor. In 2008, he was promoted to a professor of the Institute of Multidisciplinary Research for Advanced Materials, Tohoku University. In 2015, he moved to Graduate School of Bioscience and Biotechnology, Tokyo Institute of Technology. His research interests include (1) bioinpired chemistry and (2) supramolecular chemistry.

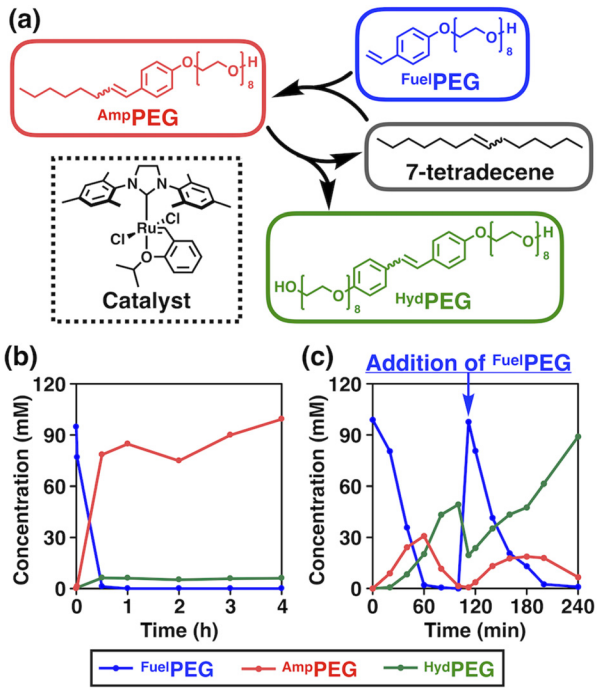

Fig. 2 (a) Schematic illustration of the designed non-equilibrium chemical reaction system based on olefin metathesis. (b) Concentration *vs.* time plot of the homogeneous reaction mixture using CH_2Cl_2 as a solvent at 25 °C (480 rpm). (c) Concentration *vs.* time plot of the biphasic reaction mixture using H_2O as a solvent at 50 °C (480 rpm). At 100 min, ^{Fuel}**PEG** was added as an additional "fuel".

resulting amphiphilic metathesis product ^{Amp}**PEG** would possess the same hydrophobic–hydrophilic balance as Triton X-114 (Fig. 1) in terms of its constituent atoms. The synthesized 7-tetradecene, ^{Fuel}**PEG**, ^{Amp}**PEG**, and ^{Hyd}**PEG** (*vide infra*) were unambiguously characterized by NMR and high-resolution mass spectrometry (Fig. S1–S13, see the ESI†).

First, we mixed 7-tetradecene, ^{Fuel}**PEG**, and Hoveyda–Grubbs catalyst 2nd generation (HG-II)[46,55,56] in CH_2Cl_2 and monitored the reaction progress using ultra-performance liquid chromatography (UPLC) (Fig. S14a, see the ESI†). Note that all reagents were uniformly dissolved so that the reaction was performed under homogeneous conditions. As shown in Fig. 2b, the concentration of ^{Amp}**PEG** (Fig. 2b, red) increased monotonically in response to the consumption of ^{Fuel}**PEG** (Fig. 2b, blue), representing the conventional reaction kinetics. Next, we used water instead of CH_2Cl_2 as a solvent to perform the same reaction under biphasic conditions (Fig. S14b, see the ESI†). Intriguingly, the reaction showed non-equilibrium kinetics where the concentration of ^{Amp}**PEG** (Fig. 2c, red) reached its maximum at 60 min and then gradually decreased. In addition, the hydrophilic metathesis product ^{Hyd}**PEG** (Fig. 2c, green) started to appear after 20 min, following the generation of ^{Amp}**PEG**. At 100 min, we observed the complete consumption of ^{Amp}**PEG** and the exclusive formation of ^{Hyd}**PEG**. These results demonstrate that ^{Amp}**PEG** was formed as a transient product, while ^{Hyd}**PEG** was formed as an accumulating "waste" product. We also added ^{Fuel}**PEG** to the reaction mixture as an additional "fuel" after the complete consumption of ^{Amp}**PEG** at 100 min and again observed the transient formation of ^{Amp}**PEG** (Fig. 2c, red), clearly demonstrating the repeatability of the designed reaction system. Note that the apparent decrease in ^{Hyd}**PEG** at 100 min (Fig. 2c, green) is due to the dilution of the reaction mixture upon addition of the aqueous solution of ^{Fuel}**PEG** (see the ESI†).

In the previous study by Fletcher and coworkers, they reported that the ruthenium catalyst was compartmentalized

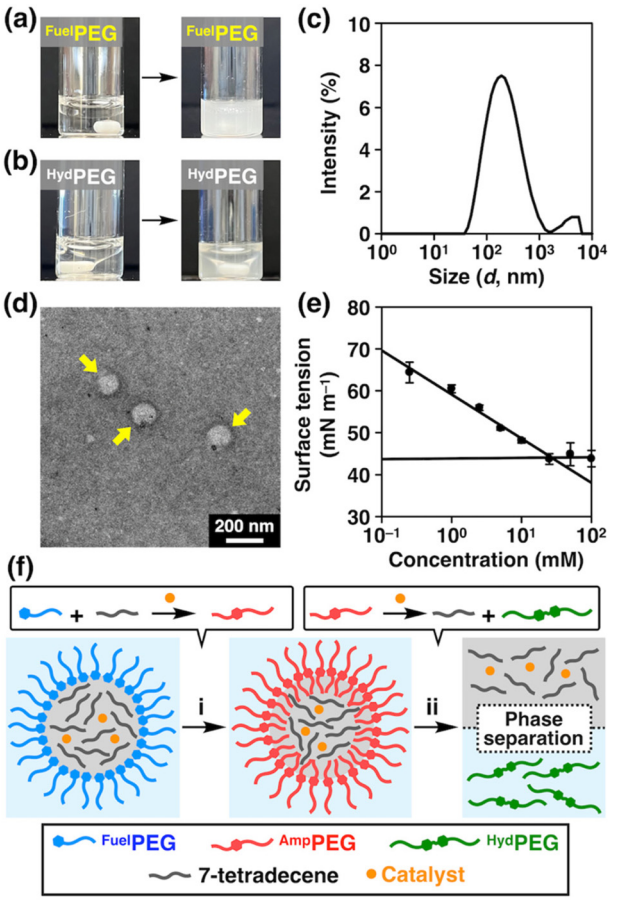

Fig. 3 (a and b) Photographs of the mixtures of 7-tetradecene and (a) aqueous ^{Fuel}**PEG** (50 mM) and (b) aqueous ^{Hyd}**PEG** (50 mM) before (left) and after (right) stirring for 4 h at 25 °C. (c) An intensity-based particle size distribution profile of aqueous ^{Fuel}**PEG** (30 mM) at 20 °C, analyzed by dynamic light scattering. The mean hydrodynamic diameter of the particle: 222.2 nm. (d) Transmission electron micrograph of aqueous ^{Fuel}**PEG** stained with gadolinium acetate. (e) Surface tension *vs.* concentration plot of aqueous ^{Fuel}**PEG**. The critical aggregation concentration (CAC) was determined from the intersection of the fitted lines ($[^{Fuel}\text{PEG}]_{CAC}$ = 26.7 mM). (f) Schematic illustration of the mechanism of the out-of-equilibrium chemical reaction. First, hydrophobic 7-tetradecene and the catalyst are surrounded by ^{Fuel}**PEG** in water. Then, the cross-metathesis reaction between 7-tetradecene and ^{Fuel}**PEG** occurs at the interface to form ^{Amp}**PEG**. Subsequently, hydrophilic ^{Hyd}**PEG** is formed and diffuses out of the interface. As a result, the reaction equilibrium is shifted, leading to the complete consumption of ^{Amp}**PEG**. Note that 7-tetradecene acts as both a reactant and an organic phase.

within the droplet of hydrophobic alkene, and cross-metathesis reactions of hydrophobic and hydrophilic alkene occurred at the interface with water.[36,46] We hypothesized that a similar reaction mechanism also took place in our system and performed qualitative kinetic simulations. In fact, the simulation for the biphasic conditions showed that the concentration of ^{Amp}PEG increased and then decreased while that for the homogeneous conditions did not (Fig. S15, see the ESI†).

Regarding the reaction mechanism, we also tested the emulsifying properties of ^{Fuel}PEG and ^{Hyd}PEG by mixing their aqueous solution with 7-tetradecene. As shown in Fig. 3a, ^{Fuel}PEG formed turbid dispersions, while ^{Hyd}PEG resulted in the much-less turbid phase-separated mixture (Fig. 3b). The difference in turbidity was also quantified by measuring the optical density (O.D.) at 600 nm (Fig. S17†). These results demonstrated that ^{Fuel}PEG could stabilize the emulsions due to its amphiphilicity, while ^{Hyd}PEG could not, likely because ^{Hyd}PEG is too hydrophilic. In fact, using dynamic light scattering (DLS, Fig. 3c), transmission electron microscopy (Fig. 3d), and surface tension measurements (Fig. 3e), we confirmed that ^{Fuel}PEG can self-assemble into spherical aggregates in water while ^{Hyd}PEG cannot (Fig. S19b†). In addition, we performed an optical microscopic observation of the emulsions formed by 7-tetradecene and ^{Fuel}PEG in the presence of HG-II and found that the interior of the emulsions were colored green (Fig. S20†), which is characteristic of the ruthenium catalyst.[57] This result indicates that HG-II was compartmentalized within the droplets of the emulsions as proposed by Fletcher and coworkers in their earlier study.[46] Considering all these results, it seems that the cross-metathesis reaction between 7-tetradecene and ^{Fuel}PEG occurred predominantly to generate ^{Amp}PEG in the early stage (Fig. 3f-i). Later, ^{Hyd}PEG was generated but then diffused out of the interface due to its hydrophilicity, and as a result, ^{Hyd}PEG was excluded from the reaction system, and the reaction equilibrium was further shifted to lead to the complete consumption of ^{Amp}PEG (Fig. 3f-ii).

With the newly developed non-equilibrium chemical reaction system in hand, we then investigated its potential to exhibit the biologically relevant properties arising from the structural similarity of ^{Amp}PEG to Triton X-114. As model cell membranes, we prepared giant unilamellar vesicles (GUVs) formed by 1,2-dioleoyl-*sn-glycero*-3-phosphocholine (DOPC) by the electroformation method (see the ESI†) and added an aliquot of the reaction mixture at different time points. We used DiIC$_{18}$(3) to label the GUVs to observe their morphologies by fluorescence microscopy. Strikingly, we observed a distinct time-dependent effect; we clearly observed GUVs when we added the reaction mixture with reaction times of 1 min (Fig. 4a, right) and 120 min (Fig. 4a, left), but we did not observe any GUVs with a reaction time of 60 min (Fig. 4a, middle). To quantitatively analyze this phenomenon, we prepared DOPC large unilamellar vesicles (LUVs) encapsulating 5-carboxyfluorescein (5-CF) by the extrusion method and examined the release of 5-CF (see the ESI†). Note that fluorescence quenching of 5-CF occurs when its concentration is high, so an increase in fluorescence intensity will be observed when it is released from inside the LUVs.[15,58–60] Using authentic samples of ^{Fuel}PEG, ^{Amp}PEG, and ^{Hyd}PEG, we confirmed that

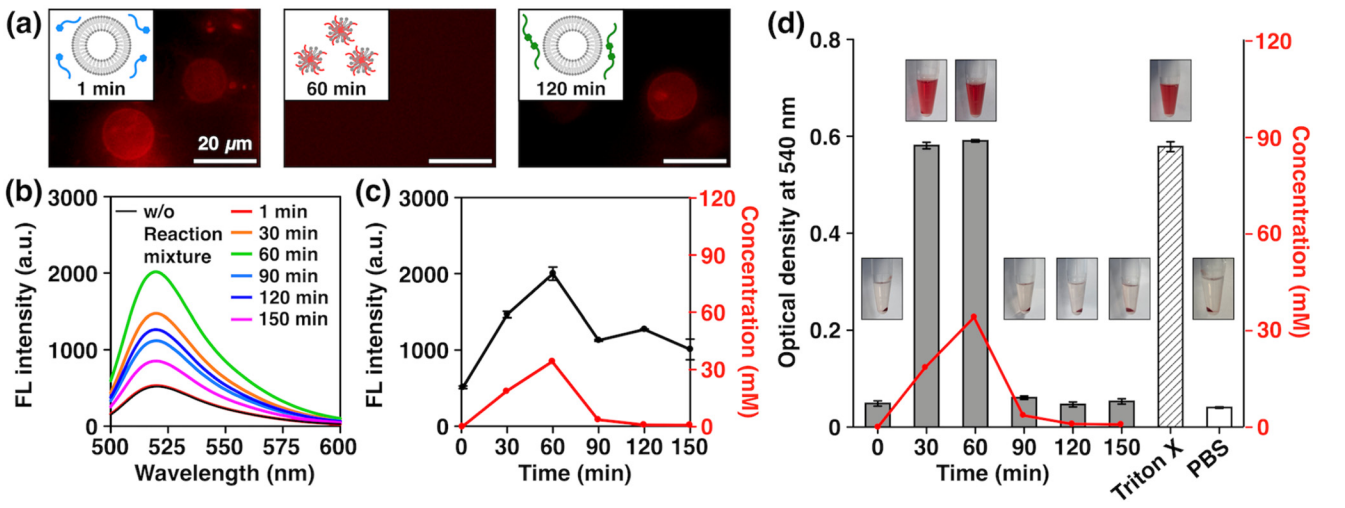

Fig. 4 (a) Fluorescence micrographs of DiIC$_{18}$(3)-labeled GUVs ([DOPC] = 600 μM, [DiIC$_{18}$(3)] = 600 nM) in aqueous glucose (2.0 mM) after the addition of the reaction mixtures at reaction times of 1 (left), 60 (middle), and 120 min (right) at 25 °C (λ_{ex} = 520–550 nm, λ_{obsd} > 580 nm). (b) Representative fluorescence intensity changes of 5-CF encapsulated in DOPC LUVs ([DOPC] = 100 μM, [5-CF] = 50 mM) in HEPES buffer ([HEPES] = 20 mM, [NaCl] = 50 mM, pH 7.5) at 20 °C after the addition of the reaction mixtures at different reaction times (λ_{ex} = 490 nm, λ_{em} = 520 nm). (c) Overlay of fluorescence intensity changes of 5-CF at 520 nm (left axis, black) and concentration changes of ^{Amp}PEG (right axis, red) as a function of time. Error bars represent standard deviations (n = 3). (d) Overlay of optical density changes of the red blood cell (RBC) suspensions at 540 nm (left axis, black) and concentration changes of ^{Amp}PEG in the reaction mixture (right axis, red) as a function of time. Error bars represent standard deviations (n = 5). The insets show the photographs of the mixtures of RBC suspensions and reaction mixtures at different reaction times.

^{Amp}PEG effectively ruptured the LUVs, while ^{Fuel}PEG and ^{Hyd}PEG did not (Fig. S24b†). We then measured the fluorescence spectra of 5-CF at different reaction time points (Fig. 4b) and plotted their intensity. As shown in Fig. 4c, the fluorescence intensity change showed a good correlation with the concentration of ^{Amp}PEG generated during the reaction. We also performed DLS measurements of the mixtures and observed the transient size change from LUVs to smaller aggregates with a diameter of 9.0 nm at a reaction time of 60 min (Fig. S25†), similar to the size of spherical micelles formed by ^{Amp}PEG alone (Fig. S18, S19a and S26†). These results clearly demonstrated the time-dependent disruption of LUVs caused by the transient generation of ^{Amp}PEG, which co-assembled with DOPC phospholipids to form micelles (Fig. 4a middle, inset).[61,62]

To further extend the properties of our non-equilibrium chemical reaction system, we investigated the possibility of transient hemolytic activity, the disruption of red blood cells (RBCs), which is highly associated with the maintenance of homeostasis in the body.[63] We added an aliquot of the reaction mixture at different time points to the suspensions of RBCs, incubated the mixture for 30 min, centrifuged, and measured the O.D. of the supernatant at 540 nm to quantify the amount of hemoglobin released by hemolysis (see the ESI†).[64] As shown in Fig. 4d, the O.D. values showed a clear correlation with the concentration of ^{Amp}PEG generated during the reaction, where high hemolytic activity was observed at the reaction time points of 30 and 60 min. Using authentic samples of ^{Fuel}PEG, ^{Amp}PEG, and ^{Hyd}PEG, we confirmed that ^{Amp}PEG is the only hemolytically active compound besides ^{Fuel}PEG and ^{Hyd}PEG (Fig. S27†). These results clearly demonstrated the first example of transient control of lytic activity by a non-equilibrium reaction system. We also analyzed the absorption spectra of the mixture and found that the denaturation of hemoglobin did not occur (Fig. S28†), which nicely corresponds to the membrane-specific activity of Triton X as mentioned earlier.[65]

Conclusions

We have newly developed a non-equilibrium chemical reaction system that generates a Triton X-mimetic amphiphile ^{Amp}PEG as a kinetic product. Through a quantitative assay using dye-embedded LUVs, we confirmed that the generation of ^{Amp}PEG enabled time-dependent membrane disruption through interaction with phospholipids. Furthermore, we demonstrated that the chemical reaction system is applicable to transient control of the resulting lytic activity. In fact, we successfully achieved time-controlled hemolysis of RBCs without denaturing hemoglobin. Although further optimization is needed to realize *in situ* control of biological activity, we believe this work has opened the door to the development of next-generation functional supramolecular materials that can precisely and temporally modulate biological events.

Author contributions

The manuscript was written through contributions of all authors. All authors have given approval to the final version of the manuscript.

Conflicts of interest

The authors declare no competing financial interest.

Acknowledgements

This work was supported by Grant-in-Aid for Scientific Research on Innovative Areas "Molecular Engine" (18H05418, 18H05419, and 23H05418 to K.K.), a Grant-in-Aid for Challenging Research (Pioneering) (23K17363 to K.K.), a Grant-in-Aid for Scientific Research (B) (23H02080 to K.S.), a Grant-in-Aid for Challenging Research (Exploratory) (23K17973 to K.S.), and a Grant-in-Aid for Transformative Research Areas "Molecular Cybernetics" (23H04408 to K. S.). K. S. also thanks The Salt Science Research Foundation, Iketani Science and Technology Foundation, The Ube Foundation, and The Mitsubishi Foundation for their financial support. The authors thank Suzukakedai Materials Analysis Division, Open Facility Center, Tokyo Institute of Technology, for NMR spectroscopy, EI mass spectrometry, ESI-TOF mass spectrometry, TEM observations, and surface tension measurements. In addition, we acknowledge Yuka Akimoto for her assistance with TEM. We thank the Open Research Facilities for Life Science and Technology, Tokyo Institute of Technology, for the use of a plate reader and an autoclave machine. We also thank Prof. Atsushi Maruyama for the use of an ultracentrifuge.

References

1 L. Milanesi and S. Tomas, *Annu. Rep. Prog. Chem., Sect. B*, 2010, **106**, 477–469.
2 K. Ruiz-Mirazo, C. Briones and A. de la Escosura, *Chem. Rev.*, 2014, **144**, 285–366.
3 B. C. Buddingh' and J. C. M. van Hest, *Acc. Chem. Res.*, 2017, **50**, 769–777.
4 P. L. Anelli, N. Spencer and J. F. Stoddart, *J. Am. Chem. Soc.*, 1991, **113**, 5131–5133.
5 M. R. Ghadiri, J. R. Granja and L. K. Buehler, *Nature*, 1994, **369**, 301–304.
6 N. Koumura, R. W. J. Zijlstra, R. A. van Delden, N. Harada and B. L. Feringa, *Nature*, 1999, **401**, 152–155.
7 V. Percec, A. E. Dulcey, V. S. K. Balagurusamy, Y. Miura, J. Smidrkal, M. Peterca, S. Nummelin, U. Edlund, S. D. Hudson, P. A. Heiney, H. Duan, S. N. Magonov and S. A. Vinogradov, *Nature*, 2004, **430**, 764–768.
8 M. S. Masar, N. C. Gianneschi, C. G. Oliveri, C. L. Stern, S. T. Nguyen and C. A. Mirkin, *J. Am. Chem. Soc.*, 2007, **129**, 10149–10158.

9 H. J. Yoon, J. Kuwabara, J.-H. Kim and C. A. Mirkin, *Science*, 2010, **330**, 66–69.
10 B. Lewandowski, G. De Bo, J. W. Ward, M. Papmeyer, S. Kuschel, M. J. Aldegunde, P. M. E. Gramlich, D. Heckmann, S. M. Goldup, D. M. D'Souza, A. E. Fernandes and D. A. Leigh, *Science*, 2013, **339**, 189–193.
11 S. Erbas-Cakmak, D. A. Leigh, C. T. McTernan and A. L. Nussbaumer, *Chem. Rev.*, 2015, **115**, 10081–10206.
12 J.-C. Chang, S.-H. Tseng, C.-C. Lai, Y.-H. Liu, S.-M. Peng and S.-H. Chiu, *Nat. Chem.*, 2016, **9**, 128–134.
13 G. De Bo, M. A. Y. Gall, S. Kuschel, J. De Winter, P. Gerbaux and D. A. Leigh, *Nat. Nanotechnol.*, 2018, **13**, 381–385.
14 S.-P. Zheng, L.-B. Huang, Z. Sun and M. Barboiu, *Angew. Chem., Int. Ed.*, 2021, **60**, 566–597.
15 K. Sato, R. Sasaki, R. Matsuda, M. Nakagawa, T. Ekimoto, T. Yamane, M. Ikeguchi, K. V. Tabata, H. Noji and K. Kinbara, *J. Am. Chem. Soc.*, 2022, **144**, 11802–11809.
16 U. Koert, M. M. Harding and J.-M. Lehn, *Nature*, 1990, **346**, 339–342.
17 B. Hasenknopf and J.-M. Lehn, *Helv. Chim. Acta*, 1996, **79**, 1643–1650.
18 J. H. K. K. Hirschberg, L. Brunsveld, A. Ramzi, J. A. J. M. Vekemans, R. P. Sijbesma and E. W. Meijer, *Nature*, 2000, **407**, 167–170.
19 H. Goto, H. Katagiri, Y. Furusho and E. Yashima, *J. Am. Chem. Soc.*, 2006, **128**, 7176–7178.
20 Q. Gan, C. Bao, B. Kauffmann, A. Grélard, J. Xiang, S. Liu, I. Huc and H. Jiang, *Angew. Chem., Int. Ed.*, 2008, **47**, 1715–1718.
21 W. Makiguchi, S. Kobayashi, Y. Furusho and E. Yashima, *Angew. Chem., Int. Ed.*, 2013, **52**, 5275–5279.
22 E. Yashima, N. Ousaka, D. Taura, K. Shimomura, T. Ikai and K. Maeda, *Chem. Rev.*, 2016, **116**, 13752–13990.
23 A. K. Dambenieks, P. H. Q. Vu and T. M. Fyles, *Chem. Sci.*, 2014, **5**, 3396–3403.
24 J. Boekhoven, W. E. Hendriksen, G. J. M. Koper, R. Eelkema and J. H. van Esch, *Science*, 2015, **349**, 1075–1079.
25 S. Maiti, I. Fortunati, C. Ferrante, P. Scrimin and L. J. Prins, *Nat. Chem.*, 2016, **8**, 725–731.
26 A. Mishra, D. B. Korlepara, M. Kumar, A. Jain, N. Jonnalagadda, K. K. Bejagam, S. Balasubramanian and S. J. George, *Nat. Commun.*, 2018, **9**, 1295.
27 K. K. Nakashima, J. F. Baaij and E. Spruijt, *Soft Matter*, 2018, **14**, 361–367.
28 E. A. J. Post and S. P. Fletcher, *Chem. Sci.*, 2020, **11**, 9434–9442.
29 J. Deng and A. Walther, *Adv. Mater.*, 2020, **32**, 2002629.
30 K. Das, L. Gabrielli and L. J. Prins, *Angew. Chem., Int. Ed.*, 2021, **60**, 20120–20143.
31 J. Flores, R. J. Brea, A. Lamas, A. Fracassi, M. Salvador-Castell, C. Xu, C. R. Baiz, S. K. Sinha and N. K. Devaraj, *Angew. Chem., Int. Ed.*, 2022, **61**, e202200549.
32 A. Sharko, D. Livitz, S. De Piccoli, K. J. M. Bishop and T. M. Hermans, *Chem. Rev.*, 2022, **122**, 11759–11777.
33 S. Bai, X. Niu, H. Wang, L. Wei, L. Liu, X. Liu, R. Eelkema, X. Guo, J. H. van Esch and Y. Wang, *Chem. Eng. J.*, 2021, **414**, 128877.
34 P. S. Schwarz, L. Tebcharani, J. E. Heger, P. Müller-Buschbaum and J. Boekhoven, *Chem. Sci.*, 2021, **12**, 9969–9976.
35 M. A. Cardona and L. J. Prins, *Chem. Sci.*, 2020, **11**, 1518–1522.
36 I. Colomer, A. Borissov and S. P. Fletcher, *Nat. Commun.*, 2020, **11**, 176.
37 D. Babu, R. J. H. Scanes, R. Plamont, A. Ryabchun, F. Lancia, T. Kudernac, S. P. Fletcher and N. Katsonis, *Nat. Commun.*, 2021, **12**, 2959.
38 N. Singh, G. J. M. Formon, S. De Piccoli and T. M. Hermans, *Adv. Mater.*, 2020, **32**, 1906834.
39 M. Tena-Solsona, B. Rieß, R. K. Grötsch, F. C. Löhrer, C. Wanzke, B. Käsdorf, A. R. Bausch, P. Müller-Buschbaum, O. Lieleg and J. Boekhoven, *Nat. Commun.*, 2017, **8**, 15895.
40 P. S. Schwarz, M. Tena-Solsona, K. Dai and J. Boekhoven, *Chem. Commun.*, 2022, **58**, 1284–1297.
41 R. Nguyen, L. Allouche, E. Buhler and N. Giuseppone, *Angew. Chem., Int. Ed.*, 2009, **48**, 1093–1096.
42 A. Jain, S. Dhiman, A. Dhayani, P. K. Vemula and S. J. George, *Nat. Commun.*, 2019, **10**, 450.
43 J. M. A. Carnall, C. A. Waudby, A. M. Belenguer, M. C. A. Stuart, J. J.-P. Peyralans and S. Otto, *Science*, 2010, **327**, 1502–1506.
44 M. Colomb-Delsuc, E. Mattia, J. W. Sadownik and S. Otto, *Nat. Commun.*, 2015, **6**, 7427.
45 S. M. Morrow, I. Colomer and S. P. Fletcher, *Nat. Commun.*, 2019, **10**, 1011.
46 I. Colomer, S. M. Morrow and S. P. Fletcher, *Nat. Commun.*, 2018, **9**, 2239.
47 J. B. Binder and R. T. Raines, *Curr. Opin. Chem. Biol.*, 2008, **12**, 767–773.
48 B. Bhushan, Y. A. Lin, M. Bak, A. Phanumartwiwath, N. Yang, M. K. Bilyard, T. Tanaka, K. L. Hudson, L. Lercher, M. Stegmann, S. Mohammed and B. G. Davis, *J. Am. Chem. Soc.*, 2018, **140**, 14599–14603.
49 V. Sabatino, J. G. Rebelein and T. R. Ward, *J. Am. Chem. Soc.*, 2019, **141**, 17048–17052.
50 I. Nasibullin, I. Smirnov, P. Ahmadi, K. Vong, A. Kurbangalieva and K. Tanaka, *Nat. Commun.*, 2022, **13**, 39.
51 A. Helenius and K. Simons, *Biochim. Biophys. Acta*, 1975, **415**, 29–79.
52 S. Kalipatnapu and A. Chattopadhyay, *IUBMB Life*, 2005, **57**, 505–512.
53 D. L. Abel, *Life*, 2012, **2**, 106–134.
54 D. E. Koshland Jr., *Science*, 2002, **295**, 2215–2216.
55 S. B. Garber, J. S. Kingsbury, B. L. Gray and A. H. Hoveyda, *J. Am. Chem. Soc.*, 2000, **122**, 8168–8179.
56 O. M. Ogba, N. C. Warner, D. J. O'Leary and R. H. Grubbs, *Chem. Soc. Rev.*, 2018, **47**, 4510–4544.
57 T. Matsuo, *Catalysts*, 2021, **11**, 359.

58 S. Benz, M. Macchione, Q. Verolet, J. Mareda, N. Sakai and S. Matile, *J. Am. Chem. Soc.*, 2016, **138**, 9093–9096.
59 R. Sasaki, K. Sato, K. V. Tabata, H. Noji and K. Kinbara, *J. Am. Chem. Soc.*, 2021, **143**, 1348–1355.
60 M. Mori, K. Sato, T. Ekimoto, S. Okumura, M. Ikeguchi, K. V. Tabata, H. Noji and K. Kinbara, *Chem. – Asian J.*, 2021, **16**, 147–157.
61 O. López, A. de la Maza, L. Coderch, C. López-Iglesias, E. Wehrli and J. L. Parra, *FEBS Lett.*, 1998, **426**, 314–318.
62 A. Pizzirusso, A. De Nicola, G. J. A. Sevink, A. Correa, M. Cascella, T. Kawakatsu, M. Rocco, Y. Zhao, M. Celino and G. Milano, *Phys. Chem. Chem. Phys.*, 2017, **19**, 29780–29794.
63 R. E. Mebius and G. Kraal, *Nat. Rev. Immunol.*, 2005, **5**, 606–616.
64 J.-B. Wang, Y.-M. Wang and C.-M. Zeng, *Biochem. Biophys. Res. Commun.*, 2011, **415**, 675–679.
65 W. Li, L. Lin and G. Li, *Anal. Methods*, 2014, **6**, 1082–1089.